SHOULDER

Neer Award 2016: reduced muscle degeneration and decreased fatty infiltration after rotator cuff tear in a poly(ADP-ribose) polymerase 1 (PARP-1) knock-out mouse model

Michael B. Kuenzler, MD[a,b], Katja Nuss, DVM[b], Agnieszka Karol, DVM[b],
Michael O. Schär, MD[a], Michael Hottiger, DVM, PhD[c,d], Sumit Raniga, MBChB, FRACS[a],
David Kenkel, MD[e], Brigitte von Rechenberg, DVM, ECVS[b,d],
Matthias A. Zumstein, MD[a,f],*

[a]Shoulder, Elbow and Orthopaedic Sports Medicine, Department of Orthopaedic Surgery and Traumatology, Inselspital, Bern University Hospital, University of Bern, Bern, Switzerland
[b]Musculoskeletal Research Unit (MSRU), Equine Department, Vetsuisse Faculty, University of Zürich, Zürich, Switzerland
[c]Institute of Veterinary Biochemistry and Molecular Biology, University of Zürich, Zürich, Switzerland
[d]Competence Center for Applied Biotechnology and Molecular Medicine (CABMM), Equine Department, Vetsuisse Faculty, University of Zürich, Zürich, Switzerland
[e]Department of Diagnostic and Interventional Radiology, University Hospital of Zürich, Zürich, Switzerland
[f]Shoulder & Elbow Unit, SportsClinic #1 AG, Bern, Switzerland

Background: Disturbed muscular architecture, atrophy, and fatty infiltration remain irreversible in chronic rotator cuff tears even after repair. Poly (adenosine 5′-diphosphate-ribose) polymerase 1 (PARP-1) is a key regulator of inflammation, apoptosis, muscle atrophy, muscle regeneration, and adipocyte development. We hypothesized that the absence of PARP-1 would lead to a reduction in damage to the muscle subsequent to combined tenotomy and neurectomy in a PARP-1 knockout (KO) mouse model.
Methods: PARP-1 KO and wild-type C57BL/6 (WT group) mice were analyzed at 1, 6, and 12 weeks (total n = 84). In all mice, the supraspinatus and infraspinatus muscles of the left shoulder were detached and denervated. Macroscopic analysis, magnetic resonance imaging, gene expression analysis, immunohistochemistry, and histology were used to assess the differences in PARP-1 KO and WT mice.
Results: The muscles in the PARP-1 KO group had significantly less retraction, atrophy, and fatty infiltration after 12 weeks than in the WT group. Gene expression of inflammatory, apoptotic, adipogenic, and muscular atrophy genes was significantly decreased in PARP-1 KO mice in the first 6 weeks.

*Reprint requests: Matthias A. Zumstein, MD, Inselspital, Bern University Hospital, Freiburgstrasse 18, Bern CH- 3010, Switzerland.
E-mail address: m.zumstein@me.com or m.zumstein@insel.ch (M.A. Zumstein).

Discussion: Absence of PARP-1 leads to a reduction in muscular architectural damage, early inflammation, apoptosis, atrophy, and fatty infiltration after combined tenotomy and neurectomy of the rotator cuff muscle. Although the macroscopic reaction to injury is similar in the first 6 weeks, the ability of the muscles to regenerate was much greater in the PARP-1 KO group, leading to a near-normalization of the muscle after 12 weeks.

Level of evidence: Basic Science Study; In-Vivo Animal Model

Rotator cuff tears (RCTs) cause profound and potentially irreversible structural alterations in the affected muscle. There is significant migration of inflammatory cells within the first few days of a tear, and the muscle fibers undergo apoptosis.[27,32] The infiltrate of inflammatory cells releases interleukin 1β (IL-1β) and tumor necrosis factor-α (TNF-α), which incites the inflammatory cascade.[32] These factors activate intracellular nuclear factor-κB (NF-κB), which not only induces apoptosis and muscular atrophy but also inhibits muscle regeneration.[23,32,35,42]

Profibrotic factors from the surrounding extracellular matrix[24] are released and activated. These factors are members of the transforming growth factor-β (TGF-β) superfamily and are key regulators of gene expression in muscle homeostasis.[20] They lead to the degradation of the injured muscle fibers and the clearance of cellular debris by M1 macrophages. Once the cellular debris have been evacuated, the monocytes transform into anti-inflammatory $M2_{reg}$ macrophages to support myogenesis[1] with the expression of myogenic regulatory factors (MRFs),[45] which in combination with other endocrine growth factors, instigate the development mature myocytes from precursor cells.[45]

If the tendon remains torn, unloaded, and retracted, the macrophages switch to become profibrotic $M2_a$ macrophages and reprogram myogenic precursor cells into the adipogenic pathway, with mature adipocytes infiltrating the free intermyofibrillar and intramyofibrillar spaces.[9] This phenomenon is termed fatty infiltration.[2,27] Although reloading the dynamic musculotendinous units leads to partial recovery of atrophy and retraction, fatty infiltration remains irreversible.[5,18] The degree of fatty infiltration in a chronically torn rotator cuff is a negative predictor for a successful surgical outcome.[46]

The complex interplay of molecular and cellular mechanisms that leads to potentially irreversible structural alterations in skeletal muscle is well described.[22] However, a single upstream regulator may orchestrate this molecular cascade. The discovery of such a regulator could potentially provide a future target for therapeutic interventions at the molecular level that may enhance the recovery of rotator cuff muscles after surgical repair.

Poly (adenosine 5′-diphosphate [ADP]-ribose) polymerase-1 (PARP-1), also known as ADP-ribosyltransferase (ARTD1), is a key transcription factor involved in the maintenance of cellular homeostasis.[37] It activates NF-κB transcription during the inflammatory response, which not only induces apoptosis and muscular atrophy but also inhibits muscle regeneration.[14,42] PARP-1 promotes a caspase-independent pathway of apoptosis via the apoptosis-inducing factor (AIF),[15] it regulates the expression of peroxisome proliferator-activated receptor-γ (PPAR-γ), which has a role in adipogenesis and may induce fatty infiltration of the muscle,[7] and it also induces muscular atrophy and fibrosis while depressing regenerative pathways.[17,40] Hence, PARP-1 may be the upstream regulator that orchestrates the molecular and cellular mechanisms that leads to potentially irreversible structural alterations after RCT.

We therefore hypothesized that the absence of PARP-1 would lead to a reduction in muscular architectural damage, early inflammation, atrophy, and fatty infiltration subsequent to combined tenotomy and neurectomy in an established PARP-1 knockout (KO) mouse model.[19,25] This study used macroscopic, histologic, molecular, and radiologic techniques to investigate the role of PARP-1 in regulating the potentially irreversible structural alterations after RCT.

Materials and methods

Animals

PARP-1 KO mice were originally obtained from Zhao-Qi Wang, PhD (Jena, Germany) and were crossed back into the C57BL/6 background. In these C57BL/6 mice, a PARP-1 gene fragment has been replaced by the neomycin resistance gene in between the second exon and intron (PARP-1 KO). The wild-type (WT) C57BL/6JOlaHsd mice were obtained from Harlan Laboratories (Horst, Netherlands). The animals were housed in a specific pathogen-free facility under standard enriched housing conditions. The study used female mice between the ages of 6 and 8 weeks at the time of surgery.

Study design

The study included 42 PARP-1 KO and 42 WT mice (Fig. 1). These mice underwent combined tenotomy and neurectomy of the supraspinatus (SSP) and infraspinatus (ISP) muscles. The animals in both groups were randomly assigned to three time points: 1, 6, and 12 weeks. The 1 week and 6 weeks time points included 12 animals each. These mice were then subdivided for histologic (histology group) or gene expression (polymerase chain reaction [PCR] group) analysis (n = 6 each). The 12 weeks time point contained 18 animals
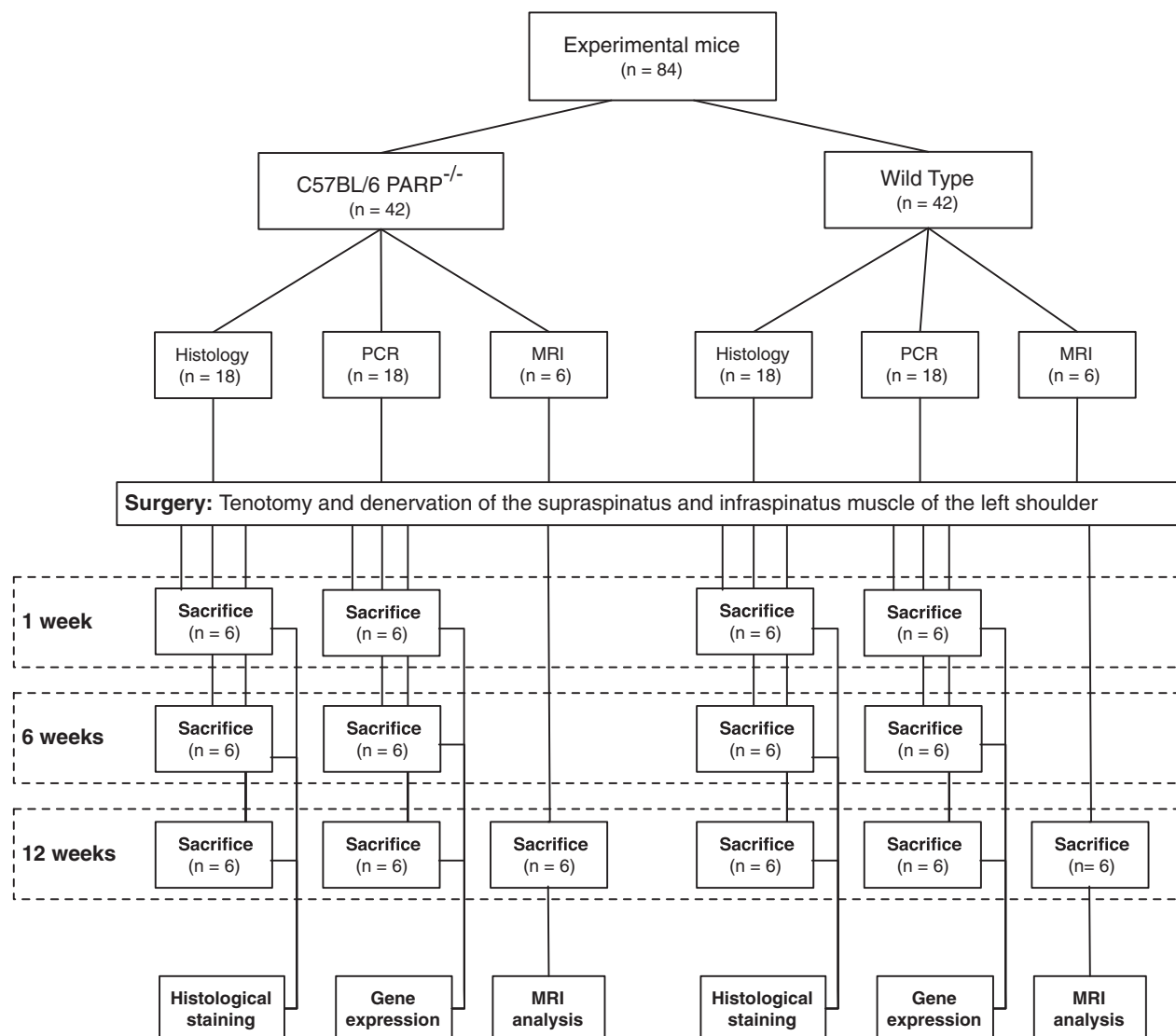
Figure 1 Flow chart of the experimental design, including the time points of surgery and euthanasia. *MRI*, magnetic resonance imaging; *PARP*^{−/−}, poly(ADP-ribose) polymerase 1 knock-out; *PCR*, polymerase chain reaction.

in each of the PARP-1 KO and WT groups. These were then further subdivided for histologic (histology group), gene expression (PCR group), or magnetic resonance imaging (MRI group) analysis (n = 6 each).

Surgery

Tenotomy and denervation of the SSP and ISP was performed according protocols published by Liu et al[25] and Kim et al.[19] Surgery was performed on the left shoulder, and the contralateral shoulder served as an uninjured control. Anesthesia was induced with an intraperitoneal administration of ketamine (30 mg/kg body weight [BW]) and maintained with inhaled isoflurane. Intraoperative pain was controlled with subcutaneous injections of buprenorphine (0.01 mg/kg BW) when indicated.

The surgical site underwent sterile preparation with chlorhexidine and draping. All procedures were performed under a surgical microscope using microsurgical instruments. A 2-cm-long skin incision was made over the shoulder joint, and the deltoid muscle was split parallel to its fibers to expose the underlying rotator cuff insertion. The deltoid was retracted with a forceps, and the tendons of the SSP and ISP were sharply detached from the humeral head. The trapezius was then split along its fibers over the lateral scapular spine. The SSP muscle was bluntly elevated to reach the suprascapular notch. The suprascapular nerve was identified, and a 2-mm segment was resected from a point where it enters the notch to a point beyond its division into supraspinatus and infraspinatus branches.

The muscular splits in the trapezius and deltoid muscles were then repaired with 10-0 Ethibond sutures (Ethicon, Somerville, NJ, USA). The skin incision was closed using staples. The animals were allowed free cage activity with food and water ad libitum postsurgery. Postoperative pain was controlled with subcutaneous injections of buprenorphine (0.01 mg/kg BW) in the first day after surgery, followed by buprenorphine (1 mL/50 mL H$_2$O) in the drinking water for 3 days.

Euthanasia and sampling

At the specified points after the intervention, the mice in the histology group were euthanized with cervical dislocation under anesthesia, followed by harvest of the entire upper extremity of both shoulders with the rotator cuff muscles intact. These samples were immediately fixed in 4% formalin. The animals in the PCR group underwent further ketamine (30 mg/kg BW) induction and anesthesia with isoflurane. The SSP and ISP muscles from both shoulders were carefully dissected and elevated from the scapula and immediately stored in RNA*later* (Qiagen, Valencia, CA, USA) at −20°C for further analysis. After the muscles were harvested, these animals were euthanized with cervical dislocation while anesthetized.

A pilot study with 6 WT mice showed severe retraction of the tendon stump in all 6 animals marked with nonabsorbable sutures, macroscopic atrophy, and fatty infiltration of the muscles 12 weeks after surgery (data not shown).

Histology

For immunohistochemistry and conventional histologic analysis, the harvested SSP and ISP muscles were fixed in 4% formalin overnight, washed with deionized water, and stored in 70% ethanol until paraffin embedding. Once embedded in paraffin, they were sectioned, deparaffinized, rehydrated in xylene and ethanol, and then incubated with specific antibodies. For routine histology, hematoxylin and eosin (H&E) and Picrosirius Red staining was performed according to institutional standard operating procedure. The slides were digitalized with a NanoZoomer 2.0-HT Digital slide scanner C9600 (Hamamatsu Photonics K.K., Hamamatsu City, Japan) in various magnifications to allow further digital processing and analysis.

To visualize intramuscular fat deposition, the midportions of SSP cross-sections were stained with a rabbit anti-mouse antibody against fatty acid binding protein 4 (Fabp4, (HPA002188; Sigma-Aldrich, St. Louis, MO, USA). Fatty infiltration, measured by the deposition of adipocytes between the muscle fiber bundles (perimysial) or within the muscle bundles due to replacement of muscle fibers (endomysial), was graded from 0 to 5 (0 = no intramuscular fat except around the main vessel; 1 = single intramuscular fat cells or fat cells that penetrate from the vessel into the muscle; 2 = streaks of fat cells into the muscle; 3 = fatty streaks in 2 of 4 quadrants of the muscle; 4 = fat cells in all quadrants; 5 = severe fatty infiltration). This cell surface marker does not differentiate between the 2 localities.

The pennation angle was measured 3 times at different locations, and the mean of these measurements used for comparison in the longitudinal sections of the ISP muscle in the Picrosirius Red-stained sections at original magnification ×20. The H&E sections underwent semiquantitative analysis. The cross-section of the SSP muscle was divided into 4 quadrants, and 4 images at original magnification ×20 magnification were taken from each quadrant and analyzed for the frequency of inflammatory cell infiltrate, degenerative cells (hypereosinophilic staining, cell swelling, fragmentation, presence of retraction caps), regenerative cells (rows of myoblast nuclei, cytoplasmic basophilia, internal nuclei), muscular atrophy (rounded to angular cells, hypereosinophilic sarcoplasm, crowded nuclei), fibrosis, and fat deposition by a veterinary pathologist who was blinded to the sample group.

Gene expression

The entire SSP samples for real-time quantitative PCR (RTqPCR) were stored in RNA*later* at −20°C until RNA extraction. The TrizolPlus Kit (Life Technologies, Carlsbad, CA, USA) was used for RNA extraction. The samples were homogenized in 1 mL Trizol per 100 mg tissue using a MixerMill (Qiagen). After homogenization, RNA was isolated by phase separation with 0.2 mL chloroform and incubation. The upper phase, containing the RNA, was then transferred to a new tube, and 1 volume of 70% ethanol was added. The solution was transferred to the Spin Cartridges (Life Technologies, Carlsbad, CA, USA) for binding and washing according to the standard manufacturers' protocol, which included DNase digestion. The purified RNA was then eluted in 30 μL RNase free water. The relative amount of RNA was measured with a NanoDrop spectrophotometer (Thermo Scientific, Waltham, MA, USA), and equal amounts of RNA were reverse transcribed to complementary (c)DNA with an RNA-to-cDNA Kit (Life Technologies) according to the manufacturer's standard protocol.

RTqPCR was performed on a 7500 Fast Real-Time PCR system (Applied Biosystems, Foster City, CA, USA) using TaqMan probes with Fast Advanced Master Mix for the expression of inflammatory (NF-κB, IL-1β, TNF-α, IL-6), apoptotic (caspase 3, AIF), atrophic (forkhead box [FOX; for all TaqMan Probes (Life Technologies, Carlsbad, CA, USA)] OS1, MuRF, Atrogin1, ubiquitin-protein ligase E [Ube] 2b and 3a), regenerative (AKT, myogenic differentiation 1 [MyoD$_1$], Myf-5), fibrotic (TGF-β$_1$ and myostatin-related muscle hypertrophy), and fatty infiltration (PPAR-γ, Fabp4) genes. Glyceraldehyde 3-phosphate dehydrogenase served as the housekeeping gene and relative levels of gene expression were measured with the ΔΔCt method relative to the contralateral uninjured side.

MRI study

We acquired T1-weighted images using a rapid acquisition with relaxation enhancement (RARE) sequence for the anatomic depiction. In-phase and out-of-phase sequences were performed for the fat quantification.[33] The sequences included the following scanning parameters: in-phase (flip angle, 50°; echo time, 2.9 ms; repetition time, 200 ms), out-of-phase (flip angle, 50°; echo time, 2.2 ms; repetition time, 200 ms), and RARE T1 (flip angle, 180°, echo time, 10 ms; repetition time, 1000 ms). All data were acquired on a 4.7-T PharmaScan (Bruker Corp., Billerica, MA, USA).

A linear polarized hydrogen whole-body mouse radiofrequency coil was used. The mice were laid head first and prone on an animal bed fitted with a pad with a continuous flow of warm water to avoid cooling of the animals. The animals were anesthetized during the acquisition with isoflurane (Attane; Minrad I, Buffalo, NY, USA), and ophthalmic ointment (Vitamin A Crème; Bausch & Lomb, Steinhausen, Switzerland) was applied to protect the mice from dry eyes. With the acquired data, a region of interest analysis was done using in-house MATLAB routines (The MathWorks, Natick, MA, USA) for the fat quantification.

Statistics

Statistical analysis included analysis of variance and post hoc tests to reveal differences between the subgroups with the Fisher least significant differences test or the Mann-Whitney test for nonparametric measurements. Linear correlation was measured with the Pearson product-moment correlation coefficient. The level of

A   Macroscopic analysis

PARP1-KO   Wild Type
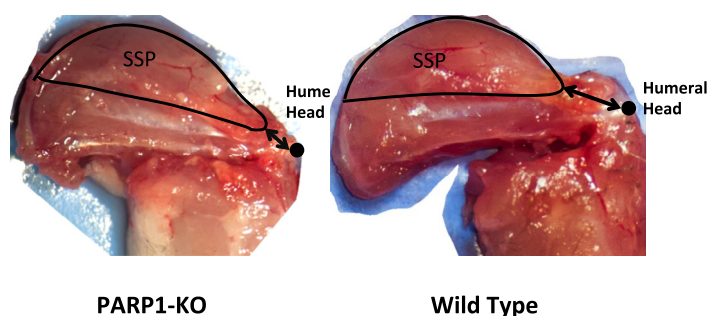
B   Radiological Retraction

PARP1-KO   Wild Type
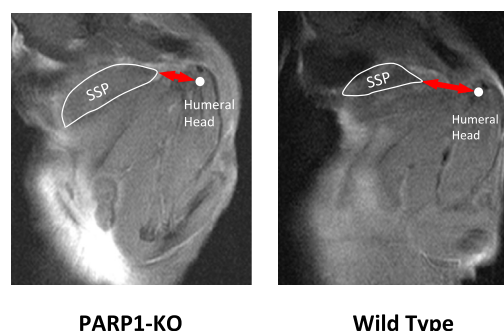
C   Muscle weight
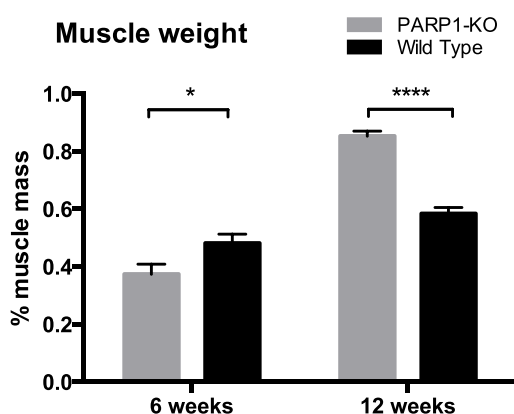
D   Retraction
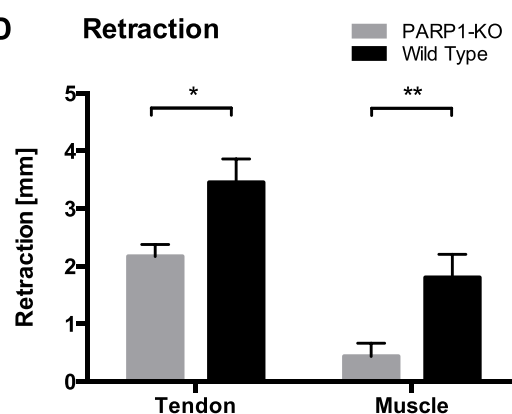
Figure 2   Results of the macroscopic and magnetic resonance imaging measurements. (**A**) Representative macroscopic images show less retraction of the tendon in poly(ADP-ribose) polymerase 1 knockout (*PARP-1 KO*) mice compared with wild-type mice. The *arrow* indicates the distance of the tendon stump to the humeral head. *SSP*, supraspinatus. (**B**) Representative images of the radiologic retraction measurements in the magnetic resonance imaging scans. The *arrow* indicates the distance of the tendon stump to the humeral head. (**C**) Muscle weight measurement. The relative weight to the contralateral uninjured side of the PARP-1 KO and wild-type mice is shown in the bar graph. (**D**) Bar graphs of the retraction measurements. Statistically significant differences are shown: *$P < .05$, **$P < .01$ and ****$P < .0001$.

significance was set to $P < .05$. Data are reported as the mean ± standard error of the mean (SEM).

Results

All animals survived the surgical procedure with no postoperative complications. All mice used their operated-on left forelimb less than the contralateral side, and the expected gait abnormality secondary to diminished use of the affected limb continued until euthanasia. No adverse effects (eg, developmental or reproductive abnormalities) were evident on examination of the PARP-1 KO mice.[43]

Macroscopic analysis

All mice in both groups showed retraction of the tendon and muscle of the SSP and ISP at 1 week, with further retraction evident at 6 weeks after combined tenotomy and neurectomy. The retraction and atrophy remained unchanged in the WT group at 12 weeks after surgery. In contrast, the PARP-1 KO mice had less retraction and almost normal muscle volume at 12 weeks. Sample images are shown in Fig. 2, *A*.

Retraction was quantified on MRI scans (Fig. 2, *B* and *D*) at 12 weeks. Tendon and muscle retraction were both significantly less in the PARP-1 KO mice compared with the WT mice ($P = .012$ and $P = .081$, respectively;, Fig. 2, *D* and Table I). The correlation between muscle and tendon retraction reached statistical significance (PARP-1 KO: $r = 0.91$, $P = .001$; WT: $r = 0.98$, $P = .0001$).

The wet weight of the SSP muscle decreased significantly in both the PARP-1 KO and in the WT mice (relative decrease compared with the uninjured contralateral side in Fig. 2, *C* and effective weight in Table I) in the first 6 weeks after combined tenotomy and neurectomy compared with the

Table I Comparison of retraction, muscle weight, and pennation angle between poly(adenosine 5'-diphosphate-ribose) polymerase 1 knockout and wild-type mice

Variable	PARP-1 knockout	Wild type	P value[*]
	Mean ± SEM	Mean ± SEM	
Retraction in MRI[†]			
Tendon, mm	2.2 ± 0.21	3.4 ± 0.41	**.012**
Muscle, mm	0.4 ± 0.23	1.8 ± 0.41	**.008**
Muscle wet weight[‡]			
6 weeks, mg	13.3 ± 3.9	12.3 ± 4.1	0.95
12 weeks, mg	31.5 ± 5.8	17.8 ± 2.5	**<.0001**

MRI, magnetic resonance imaging; *PPAR-1*, poly(adenosine 5'-diphosphate-ribose) polymerase; *SEM*, standard error of the mean.

  * Statistically significant differences (*P* < .05) are marked in bold.
  † Retraction was measured in the MRI scans after 12 weeks.
  ‡ Muscle weight values are relative to the contralateral uninjured side.

uninjured contralateral side. At 12 weeks postsurgery, the wet weight of the SSP in PARP-1 KO mice was almost normal compared with the contralateral side but remained significantly lower in the WT mice (difference *P* < .0001; Fig. 2, *C* and Table I).

Histology

Compared with the uninjured contralateral side of all animals, there was a statistically significant increase in pennation angle, in the WT mice (control: 23.9° ± 0.9°; Fig. 3, *E* and Table II; 1 week: 31.1° ± 2.4°, *P* = .016; 6 weeks: 36.1° ± 4.9°, *P* = .0002; 12 weeks: 34.4° ± 5.9°, *P* = .0014, respectively). Conversely, after an initial increase in the pennation angle in the PARP-1 KO mice, it remained unchanged at 6 and 12 weeks and did not reach statistical significance compared with the controls (1 week: 30.0° ± 3.5°, *P* = .088; 6 weeks: 28.1° ± 4.9°, *P* = .155; 12 weeks: 28.5° ± 3.9°, *P* = .103, respectively). There was a statistically significant correlation between the pennation angle and the tendon and muscle retraction measurements in the PARP-1 KO mice (*r* = 0.93, *P* = .008 and *r* = 0.9, *P* = .014, respectively) but not in the WT mice (*r* = −0.38, *P* = .517 and *r* = −0.36, *P* = .546, respectively).

H&E staining of the SSP cross-sections showed a higher inflammatory cell infiltrate at 1 week after injury in the WT mice (Fig. 3, *A*). This was followed by an increase in degenerative changes in both groups, with muscle fibers undergoing degradation and atrophy at 6 weeks. PARP-1 KO mice had a higher number of regenerating fibers at this assessment. After 12 weeks, almost no degenerative changes were observed in either group. Muscles of the PARP-1 KO group had less fibrosis and better muscle architecture compared with the WT group (Fig. 3, *D*).

Fatty infiltration

Neither group had fatty infiltration at 1 week (data not shown); however, fatty infiltration was present in both groups at 6 weeks, with an average grade of 2.7 ± 0.49 in the PARP-1 KO mice and 2.3 ± 0.49 in the WT mice (*P* = .818 for difference; Fig. 3, *B* and *C*). This almost significantly decreased in the PARP-1 KO mice to 1.4 ± 0.25 at 12 weeks postsurgery (*P* = .082), which was significantly lower than in the WT mice (2.8 ± 0.37; *P* = .032 for difference). Intramuscular fat was also quantified in the in-phase and opposed-phase of the MRI scans. The relative amount of intramuscular fat was significantly lower in the PARP-1 KO group (12.5% ± 1.82%) compared with the WT group (19.6% ± 1.96%; *P* = .027 for difference).

Gene expression analysis

Gene expression analysis of various inflammatory genes revealed that TNF-α messenger RNA (mRNA) was upregulated at 1 and 12 weeks after injury in both PARP-1 KO and WT mice without reaching statistical significance (*P* = .775 and *P* = .390, respectively; Fig. 4, *A*). IL-1β expression was upregulated at 1 and 6 weeks after surgery in the WT group, without reaching statistical significance compared with the PARP-1 KO mice (1 week: *P* = .197, 6 weeks: *P* = .110). There was a significant upregulation of NF-κB (*P* < .0001) and the proapoptotic factor AIF (*P* = .005) at 1 week in the WT group.

The proliferative factors TGF-β$_1$ and myostatin also had significantly upregulated mRNA in the WT group at 1 week (*P* < .0001 and *P* = .0038, respectively; Fig. 4, *B*). The muscle atrophy-related ubiquitin ligases muscle RING finger 1 (MuRF1) and atrogin-1 were present at significantly (*P* = .048 and *P* = .0018, respectively) higher levels in the WT group, consistent with the higher levels of Ube3a mRNA at 1 week (*P* < .0001; Fig. 4, *C*). The mRNA level of regulatory protein FOXO3 was also significantly upregulated in the WT mice at 6 weeks (*P* = .013, Fig. 4, *C*).

AKT, the main regulator of muscle regeneration, was equally upregulated in the PARP-1 KO and WT groups at 1 and 12 weeks (*P* = .447 and *P* = .990 respectively; Fig. 4, *D*). MyoD and Myf-5 mRNA were both upregulated at weeks 1 and 6 after surgery in both groups. The upregulation of both factors was significantly higher at week 1 in the WT group than in the PARP-1 KO group (*P* = .0053 and *P* = .012, respectively; Fig. 4, *D*). The mRNA levels of genes regulating fatty infiltration were significantly upregulated at 6 weeks in the WT group (PPAR-γ: *P* = .012, Fabp4: *P* = .0124; Fig. 4, *E*).

Discussion

Disturbed muscular architecture, complete atrophy, and fatty infiltration remain irreversible in chronic RCTs even after repair. The complex interplay of molecular and cellular mechanisms, which leads to potentially irreversible structural
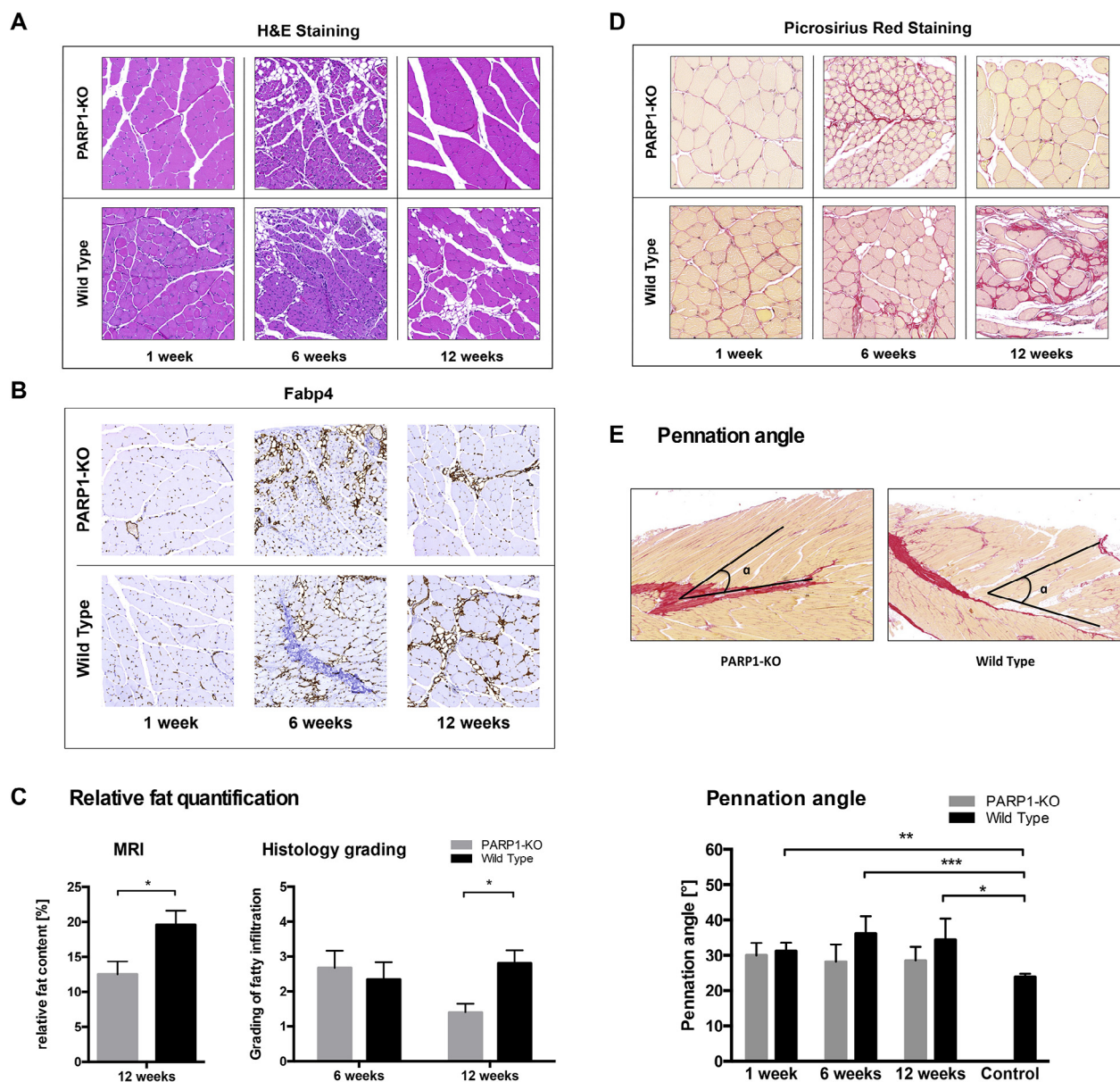
Figure 3 Representative histologic slides and results of the fat quantification and pennation angle measurement. (**A**) Representative histologic cross-sections of the supraspinatus (*SSP*) stained with hematoxylin and eosin (*H&E*) after 1, 6 and 12 weeks. (**B**) Representative histologic cross-sections stained with an antibody against Fabp4. (**C**) Fat quantification in the SSP muscles. Relative fat quantification in the magnetic resonance imaging (MRI) scans with a 2-point Dixon method on a 4.7-T small-animal MRI scanner and histologic grading of the endomysial and perimysial fat content in the cross sections of the SSP muscles stained with Fabp4. (**D**) Representative histologic cross-sections of the SSP stained with Picrosirius Red to visualize the connective tissue. (**E**) Pennation angle measurements in the Picrosirius Red stained longitudinal sections of the infraspinatus (*ISP*) muscles of poly(ADP-ribose) polymerase 1 knockout (*PARP-1*) and wild-type mice and bar graphs indicating the degree of the angle. The contralateral side of both groups acted as an uninjured control measurement. Original magnification: parts A, B, and D x20; part E x5. Statistically significant differences are shown: *$P < .05$, **$P < .01$, and ***$P < .001$.

alterations in skeletal muscle, has been described.[22] PARP-1, also known ARTD1, is a key transcription factor involved in the maintenance of cellular homeostasis.[21] PARP-1 has shown to be a key regulator of inflammation, apoptosis, muscle atrophy, muscle regeneration, and adipocyte development.[7,14,40] Our study is the first to show that the absence of PARP-1 leads to a reduction in muscular architectural damage in the su-

praspinatus and infraspinatus muscle of mice. PARP-1 may be the upstream regulator that orchestrates the molecular and cellular mechanisms that leads to these potentially irreversible structural alterations after RCT.

Macroscopic analysis showed different degrees of tendon and muscle retraction in both WT and PARP-1 KO mice at 1 and 6 weeks after combined tenotomy and neurectomy. After

Table II Comparison of the pennation angle in the infraspinatus between poly(adenosine 5'-diphosphate-ribose) polymerase 1 knock-out, wild-type mice, and uninjured control site

Variable[*]	Overall	1 week	6 weeks	12 weeks
Controls[†]	23.8° ± 0.9°			
P value vs. control		.080	.160	.100
PARP-1 knockout		30.0° ± 3.5°	28.1° ± 4.9°	28.5° ± 3.9°
Wild type		31.1° ± 2.4°	36.1° ± 4.9°	34.4° ± 5.9°
P value vs. control[‡]		**.017**	**.0002**	**.0014**

PARP-1, poly(ADP-ribose) polymerase 1.

  * Values are mean ± standard error of the mean.
  † The contralateral uninjured infraspinitus muscles served as controls.
  ‡ Statistically significant differences (*P* < .05) are marked in bold.

12 weeks, retraction of the tendon and muscle was significantly lower in the PARP-1 KO mice than in the WT mice measured in MRI scans. In a 2006 sheep study, Meyer et al[31] also showed that the tendon retracts more than muscle in experimental chronic RCTs. This results in an apparently shortened tendon. In our study, despite the degree of fatty infiltration being less than 50% of the muscle volume (Goutallier stage <3) in all animals, the degree of tendon retraction was consistently much greater than muscle retraction.

Liu et al[25] observed significant and consistent muscle atrophy after rotator cuff tendon transection in a mouse model. Furthermore, they found that denervation significantly increased the amount of muscle atrophy after a RCT in a mouse model.[25] Muscle atrophy persisted in the WT group in our study, but the PARP-1 KO mice had almost normal muscle volume at 12 weeks. This occurrence was further supported by near-normalization of the wet weight of the SSP in PARP-1 KO mice but remained low in the WT mice after the initial decrease in both groups. Only after continuous elongation and subsequent refixation do retracted, fatty infiltrated, and atrophied rotator cuff muscles in sheep achieve partial reversal of muscle atrophy but not fatty infiltration.[10]

Meyer et al[30] described the pathomechanical concept of the pennation angle to explain muscle loss and fatty infiltration after RCT. Geometric modeling showed that the increase of the pennation angle separates the muscle fiber bundles mechanically like limbs of a parallelogram. Infiltrating fat cells fill the created space between the reoriented muscle fibers, which may be quantitatively calculated without affecting the structural properties of the muscle cells. Our histologic data were consistent with the macroscopic findings. Both groups in our study demonstrated an increase in the pennation angle at 1 week after combined tenotomy and neurectomy. The pennation angle further increased in the WT mice at 6 weeks and remained high at 12 weeks but remained unchanged in the PARP-1 KO mice at 6 and 12 weeks. In contrast to the WT group, the increase in the pennation angle in the PARP-1 KO mice did not reach statistical significance compared with the controls at any time point.

Fatty infiltration was present in both groups at 6 weeks. The infiltration decreased in the PARP-1 KO mice to 1.4 ± 0.25 at 12 weeks postsurgery, which was significantly lower than in the WT mice, where the grading conversely increased to 2.8 ± 0.37 from 6 weeks. The MRI measurement of relative intramuscular fat was also significantly lower in the PARP-1 KO group at 12 weeks. Gerber et al[10] demonstrated an arrest of fatty infiltration after continuous elongation and refixation in a sheep model.

A study in sheep[11] found that neither an anabolic steroid nor insulin-like growth factor contributed to regeneration of the muscle once degenerative changes were established. The findings demonstrated that muscle cells lose reactiveness to an anabolic steroid and insulin-like growth factor once retraction has led to fatty infiltration and atrophy of the muscle.[11] Treatment of mice with tamoxifen, a competitive estrogen receptor inhibitor, caused less atrophy and inflammation after RCT, but fatty infiltration remained unchanged.[4] To date, only one other published study has demonstrated reversal of fatty infiltration: through local administration of adipose-derived stem cells into repaired rabbit SSC muscle, Oh et al[34] demonstrated improvement in fatty infiltration and tendon healing. Because we had significantly less fatty infiltration and atrophy at 12 weeks in the PARP-1 KO group, one may speculate that outcome after fixation of the RCT in this group may have an improved surgical outcome.

Results of the gene expression analysis further support the hypothesis that PARP-1 may be an instrumental upstream regulator that orchestrates potentially irreversible structural alterations after RCT. Regeneration and degeneration are in harmony during normal muscle homeostasis. RCTs incite an inflammatory response that begins with inflammatory cell infiltration and subsequent release of proinflammatory cytokines.[32] Intramuscular macrophages release TNF-α and IL-1β and thereby stimulate the upregulation of NF-κB. NF-κB has an integral role in influencing muscle degeneration[23,42]: (1) it coregulates the expression of inflammatory and proapoptotic cytokines that cause muscle damage, (2) promotes muscular atrophy and degradation directly via activation of MuRF1 or indirectly via upregulation of other cytokines, and (3) it inhibits myogenic differentiation and regeneration. PARP-1 has been shown to be an important cofactor for NF-κB dependent transcription of various genes,[14] and the
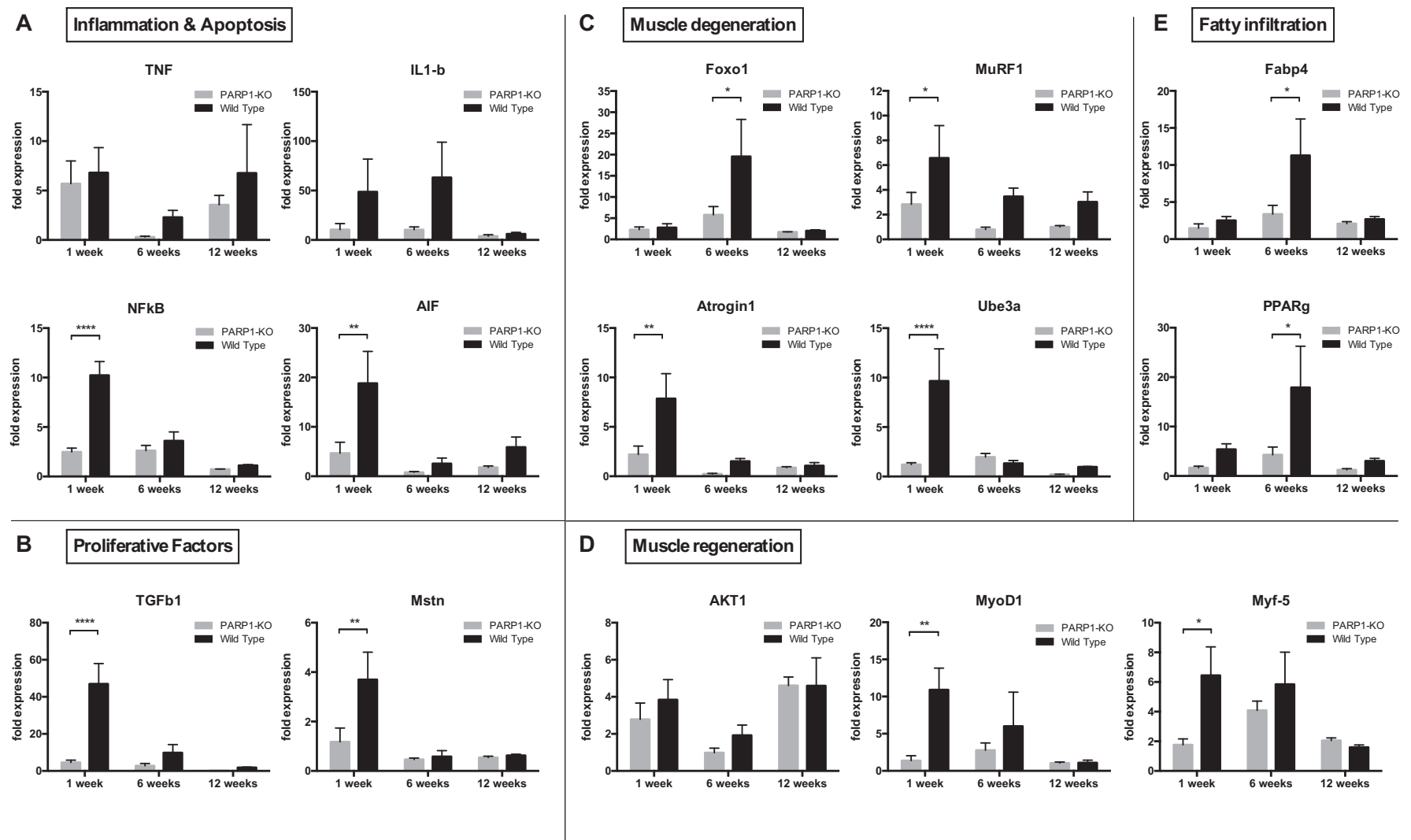
Figure 4 Results of the gene expression analysis with real-time reverse-transcriptase polymerase chain reaction in poly(ADP-ribose) polymerase 1 knockout (*PARP-KO*) and wild-type mice. The increase of messenger RNA levels is shown as fold expression compared with the uninjured contralateral side with the ΔCt method. (**A**) Genes of the inflammatory cascade (tumor necrosis factor-α [*TNF*-α], interleukin [*IL*]-1β, and nuclear factor-κB [*NF*-κB]) and apoptosis (apoptosis-inducing factor [*AIF*]). (**B**) Proliferative factors of the transforming growth factor-β (*TGF*-β) superfamily represented by TGF-β1 and myostatin. (**C**) Genes involved in the degeneration of muscle fibers. Forkhead box (*Fox*)o1 is the upstream regulator of the ubiquitin-ligases muscle atrophy-related ubiquitin ligases muscle RING finger 1 (*MuRF1*) and atrogin-1, which bind to ubiquitin-protein ligase E (*Ube*) 3a. (**D**) Genes for muscular regeneration. AKT1 is the upstream regulator of the myogenic regulatory factors here represented by MyoD1 and Myf-5. (**E**) Genes regulating fatty infiltration (peroxisome proliferator-activated receptor [*PPAR*]-γ) and binding of fatty acids (fatty acid binding protein 4 [*Fabp4*]). Statistically significant differences are shown: *$P < .05$, **$P < .01$, and ****$P < .0001$.

disturbance of this interaction leads to a lower inflammatory reaction to injury.[14] Studies have shown that inactivation or deletion of PARP-1 protects tissues from damage, as noted in the 2013 review by Kraus and Hottiger.[21]

Our results showed an inflammatory response at 1 week after combined tenotomy and neurectomy of the SSP and ISP muscles in the PARP-1 KO and the WT mice. TNF-α and IL-1β are extracellular inflammatory cytokines that induce intracellular inflammatory cascades. They were upregulated in both groups but only led to a significant upregulation of NF-κB in the muscles of WT mice. This may be explained by a dampened inflammatory response and subsequent reduction in proinflammatory cytokine expression in the muscles of PARP-1 KO mice.[13] Only the WT mice had significantly higher levels of the proapoptotic AIF, which is activated by PARP-1 and promotes caspase-independent apoptosis. AIF translocates into the nucleus where it triggers apoptosis.[44] The increase in proapoptotic gene expression suggests higher apoptosis rates in WT mice leading to a more pronounced cell death in this group.

Unloading or denervation of the musculotendinous unit initiates complex pathways that eventually result in muscle ubiquitination and degradation.[41] Ubiquitination requires ligases to form complexes with Ube3a, which allows recognition and proteosome-mediated degradation of muscle fibers.[41] The most important of these ligases are MuRF1 and atrogin-1 (FBX032).[3] Their transcription is upregulated by inflammatory, profibrotic, proadipogenic, and the FOXO transcription factors.[23,29,36,38] The key elements involved in the process of ubiquitination and muscle degradation, Ube3a, MuRF1, and atrogin-1, were all significantly upregulated in the WT mice at 1 week after combined tenotomy and neurectomy.

Satellite cells and mesenchymal stem cells are activated during muscle regeneration and undergo proliferation and differentiation.[45] This process is orchestrated by MRFs, such as MyoD and Myf-5, which are activated through the AKT/mechanistic target of rapamycin pathway.[45] In addition, NF-κB has been shown to have a direct inhibitory effect on muscular regeneration by inhibiting the MRFs, specifically MyoD.[13] This inhibition of myogenic differentiation and regeneration is also a major effect of NF-κB in muscle degeneration. We interpret the significant upregulation of MyoD in WT mice after 1 week as a failed attempt of the muscle to induce regeneration through stimulation of satellite cells and mesenchymal stem cells. Meanwhile, in the absence of PARP-1 in the KO group, NF-κB is not effective in inhibiting MyoD, and fewer muscle fibers were damaged during the initial inflammatory response. Upregulation of MyoD, as in the WT group, is not needed, and low levels of MyoD may be sufficient for regeneration of the muscle fibers, leading to a normalization of the muscle weight after 12 weeks.

Factors TGF-β_1 and myostatin were both significantly upregulated in the WT group at 1 week. The inflammatory cell infiltrate triggers the release of TGF-β_1 and myostatin from the fibroblasts in the extracellular matrix.[18,24] Both factors belong to the TGF superfamily.[20] Members of this TGF superfamily have been shown to induce fibrosis and regulate muscle mass.[28] Specifically, myostatin inhibits myogenic differentiation by downregulating the expression of MyoD and myogenin.[39] PARP-1 modulates TGF-β_1 activity via negative and positive feedback mechanisms that allow fine-tuning of these pathways.[6,26] Our data suggest that the significant early activation of TGF-β_1 transcription in WT mice directs the balance toward fibrosis and degeneration.

Our study showed fatty infiltration in both mice groups at 6 weeks but significantly less fatty infiltration in PARP-1 KO mice after 12 weeks. The proadipogenic factors PPAR-γ and fatty acid binding protein 4 both revealed a significantly higher expression in the WT mice than in the PARP-1 KO group at 6 weeks after injury. These proadipogenic genes are key factors in fat accumulation in between free inter myofibrillar and intramyofibrillar spaces and also decrease the expression of MRF.[16] In addition, myostatin and TGF-β reduce the expression of the proadipogenic factors.[12] This may be the reason PPAR-γ is only upregulated at 6 weeks, after the inhibitory effect of myostatin and TGF-β has dissipated. Furthermore, absence of PARP-1 directly inhibits the function of PPAR-γ[7,17] and is a crucial regulator of adipogenic differentiation.[8]

This study has some limitations. It could be suggested the differences observed in our study were due to reinnervation. This is not plausible for 3 reasons. Firstly, a 2-mm length of the nerve was transected from the main branch at its entrance into the scapular notch extending beyond its branches to the SSP and ISP in both the WT and PARP-1 KO mice. Secondly, were the nerves to reinnervate by chance, we would expect more outliers in our data; however, none of our data, including muscle weight measurements, demonstrate outliers with a narrow standard deviation. Thirdly, why should the reinnervation phenomena be confined to the PARP-1 KO group only and not occur in the WT group?

Another possible criticism could be that we analyzed gene expression and not effective protein levels and their activity. This does limit our ability to fully interpret the molecular mechanisms at play. We surgically transected the SSP and ISP tendons from their origin at the humeral head. This may not accurately mimic degenerative RCTs seen in the human population, but to our knowledge, there are no degenerative RCT mouse models. There are other animal models of chronic RCTs, but this would not allow us to use the PARP-1 KO model. This study relies on gene expression analysis and does not investigate the exact interactions between PARP-1 and the described proteins on a molecular level. Further molecular biological methods would be needed to describe these mechanisms. The first assessment at 1 week may be perceived as a bit delayed to assess inflammation, but we were still able to observe significant differences between the PARP-1-KO and WT mice in all of the various modes of analyses.

Conclusion

Our study is the first to show that the absence of PARP-1 leads to a reduction in muscular architectural damage, early inflammation, apoptosis, atrophy, and fatty infiltration after combined tenotomy and neurectomy of the rotator cuff muscle. PARP-1 is one of the upstream regulators that orchestrates the molecular and cellular mechanisms that leads to potentially irreversible structural alterations after RCT. It plays an important role in modulating the muscles reaction to RCT by promoting the immediate inflammatory response. This inflammatory response leads to apoptosis and damage to the muscle fibers and initiates muscular degeneration and atrophy. Architectural changes and loss of myocytes hinder the ability of muscles to regenerate and ultimately lead to fatty infiltration. In the absence of PARP-1, the initial inflammatory response is dampened, leading to less myocyte degeneration. Although the reaction of the macroscopic muscles to injury is similar in the first 6 weeks, the ability to regenerate is much greater in the PARP-1 KO group, leading to a near-normalization of muscle substance and muscle weight, less retraction, and less fatty infiltration after 12 weeks. We conclude that PARP1 is a molecular regulator of muscular deterioration after RCT.

Appendix
Supplementary data

Supplementary data to this article can be found online at http://dx.doi.org/10.1016/j.jse.2016.11.009

References

1. Arnold L, Henry A, Poron F, Baba-Amer Y, van Rooijen N, Plonquet A, et al. Inflammatory monocytes recruited after skeletal muscle injury switch into antiinflammatory macrophages to support myogenesis. J Exp Med 2007;204:1057-69. http://dx.doi.org/10.1084/jem.20070075

2. Barry JJ, Lansdown DA, Cheung S, Feeley BT, Ma CB. The relationship between tear severity, fatty infiltration, and muscle atrophy in the supraspinatus. J Shoulder Elbow Surg 2013;22:18-25. http://dx.doi.org/10.1016/j.jse.2011.12.014

3. Bodine SC, Latres E, Baumhueter S, Lai VK, Nunez L, Clarke BA, et al. Identification of ubiquitin ligases required for skeletal muscle atrophy. Science 2001;294:1704-8.

4. Cho E, Zhang Y, Pruznak A, Kim HM. Effect of tamoxifen on fatty degeneration and atrophy of rotator cuff muscles in chronic rotator cuff tear: an animal model study. J Orthop Res 2015;33:1846-53. http://dx.doi.org/10.1002/jor.22964

5. Choo A, McCarthy M, Pichika R, Sato EJ, Lieber RL, Schenk S, et al. Muscle gene expression patterns in human rotator cuff pathology. J Bone Joint Surg Am 2014;96:1558-65. http://dx.doi.org/10.2106/JBJS.M.01585

6. Dahl M, Maturi V, Lönn P, Papoutsoglou P, Zieba A, Vanlandewijck M, et al. Fine-tuning of Smad protein function by poly(ADP-ribose) polymerases and poly(ADP-ribose) glycohydrolase during transforming growth factor beta signaling. PLoS One 2014;9:e103651. http://dx.doi.org/10.1371/journal.pone.0103651.

7. Erener S, Hesse M, Kostadinova R, Hottiger MO. Poly(ADP-ribose)polymerase-1 (PARP1) controls adipogenic gene expression and adipocyte function. Mol Endocrinol 2012;26:79-86. http://dx.doi.org/10.1210/me.2011-1163

8. Erener S, Mirsaidi A, Hesse M, Tiaden AN, Ellingsgaard H, Kostadinova R, et al. ARTD1 deletion causes increased hepatic lipid accumulation in mice fed a high-fat diet and impairs adipocyte function and differentiation. FASEB J 2012;26:2631-8. http://dx.doi.org/10.1096/fj.11-200212

9. Frey E, Regenfelder F, Sussmann P, Zumstein M, Gerber C, Born W, et al. Adipogenic and myogenic gene expression in rotator cuff muscle of the sheep after tendon tear. J Orthop Res 2009;27:504-9. http://dx.doi.org/10.1002/jor.20695

10. Gerber C, Meyer D, Frey E, von Rechenberg B, Hoppeler H, Frigg R, et al. Neer Award 2007: reversion of structural muscle changes caused by chronic rotator cuff tears using continuous musculotendinous traction. An experimental study in sheep. J Shoulder Elbow Surg 2009;18:163-71. http://dx.doi.org/10.1016/j.jse.2008.09.003

11. Gerber C, Meyer DC, Von Rechenberg B, Hoppeler H, Frigg R, Farshad M. Rotator cuff muscles lose responsiveness to anabolic steroids after tendon tear and musculotendinous retraction: an experimental study in sheep. Am J Sports Med 2012;40:2454-61. http://dx.doi.org/10.1177/0363546512460646

12. Guo W, Flanagan J, Jasuja R, Kirkland J, Jiang L, Bhasin S. The effects of myostatin on adipogenic differentiation of human bone marrow-derived mesenchymal stem cells are mediated through cross-communication between Smad3 and Wnt/beta-catenin signaling pathways. J Biol Chem 2008;283:9136-45. http://dx.doi.org/10.1074/jbc.M708968200

13. Guttridge DC, Mayo MW, Madrid LV, Wang CY, Baldwin AS Jr. NF-kappaB-induced loss of MyoD messenger RNA: possible role in muscle decay and cachexia. Science 2000;289:2363-6.

14. Hassa PO, Hottiger MO. A role of poly (ADP-ribose) polymerase in NF-kappaB transcriptional activation. Biol Chem 1999;380:953-9.

15. Hong SJ, Dawson TM, Dawson VL. Nuclear and mitochondrial conversations in cell death: PARP-1 and AIF signaling. Trends Pharmacol Sci 2004;25:259-64. http://dx.doi.org/10.1016/j.tips.2004.03.005

16. Hu E, Tontonoz P, Spiegelman BM. Transdifferentiation of myoblasts by the adipogenic transcription factors PPAR gamma and C/EBP alpha. Proc Natl Acad Sci U S A 1995;92:9856-60.

17. Huang D, Wang Y, Wang L, Zhang F, Deng S, Wang R, et al. Poly(ADP-ribose) polymerase 1 is indispensable for transforming growth factor-beta Induced Smad3 activation in vascular smooth muscle cell. PLoS One 2011;6:e27123. http://dx.doi.org/10.1371/journal.pone.0027123.

18. Killian ML, Lim CT, Thomopoulos S, Charlton N, Kim HM, Galatz LM. The effect of unloading on gene expression of healthy and injured rotator cuffs. J Orthop Res 2013;31:1240-8. http://dx.doi.org/10.1002/jor.22345

19. Kim HM, Galatz LM, Lim C, Havlioglu N, Thomopoulos S. The effect of tear size and nerve injury on rotator cuff muscle fatty degeneration in a rodent animal model. J Shoulder Elbow Surg 2012;21:847-58. http://dx.doi.org/10.1016/j.jse.2011.05.004

20. Kollias HD, McDermott JC. Transforming growth factor-beta and myostatin signaling in skeletal muscle. J Appl Physiol 2008;104:579-87. http://dx.doi.org/10.1152/japplphysiol.01091.2007

21. Kraus WL, Hottiger MO. PARP-1 and gene regulation: progress and puzzles. Mol Aspects Med 2013;34:1109-23. http://dx.doi.org/10.1016/j.mam.2013.01.005

22. Laron D, Samagh SP, Liu X, Kim HT, Feeley BT. Muscle degeneration in rotator cuff tears. J Shoulder Elbow Surg 2012;21:164-74. http://dx.doi.org/10.1016/j.jse.2011.09.027

23. Li H, Malhotra S, Kumar A. Nuclear factor-kappa B signaling in skeletal muscle atrophy. J Mol Med 2008;86:1113-26. http://dx.doi.org/10.1007/s00109-008-0373-8

24. Liu X, Joshi SK, Ravishankar B, Laron D, Kim HT, Feeley BT. Upregulation of transforming growth factor-beta signaling in a rat model of rotator cuff tears. J Shoulder Elbow Surg 2014;23:1709-16. http://dx.doi.org/10.1016/j.jse.2014.02.029

25. Liu X, Laron D, Natsuhara K, Manzano G, Kim HT, Feeley BT. A mouse model of massive rotator cuff tears. J Bone Joint Surg Am 2012;94:e41. http://dx.doi.org/10.2106/JBJS.K.00620

26. Lönn P, van der Heide LP, Dahl M, Hellman U, Heldin CH, Moustakas A. PARP-1 attenuates Smad-mediated transcription. Mol Cell 2010;40:521-32. http://dx.doi.org/10.1016/j.molcel.2010.10.029

27. Lundgreen K, Lian OB, Engebretsen L, Scott A. Tenocyte apoptosis in the torn rotator cuff: a primary or secondary pathological event? Br J Sports Med 2011;45:1035-9. http://dx.doi.org/10.1136/bjsm.2010.083188

28. McPherron AC, Lawler AM, Lee SJ. Regulation of skeletal muscle mass in mice by a new TGF-beta superfamily member. Nature 1997;387:83-90.

29. Mendias CL, Gumucio JP, Davis ME, Bromley CW, Davis CS, Brooks SV. Transforming growth factor-beta induces skeletal muscle atrophy and fibrosis through the induction of atrogin-1 and scleraxis. Muscle Nerve 2012;45:55-9. http://dx.doi.org/10.1002/mus.22232

30. Meyer DC, Hoppeler H, von Rechenberg B, Gerber C. A pathomechanical concept explains muscle loss and fatty muscular changes following surgical tendon release. J Orthop Res 2004;22:1004-7. http://dx.doi.org/10.1016/j.orthres.2004.02.009

31. Meyer DC, Lajtai G, von Rechenberg B, Pfirrmann CW, Gerber C. Tendon retracts more than muscle in experimental chronic tears of the rotator cuff. J Bone Joint Surg Br 2006;88:1533-8. http://dx.doi.org/10.1302/0301-620x.88b11.17791

32. Millar NL, Hueber AJ, Reilly JH, Xu Y, Fazzi UG, Murrell GA, et al. Inflammation is present in early human tendinopathy. Am J Sports Med 2010;38:2085-91. http://dx.doi.org/10.1177/0363546510372613

33. Nozaki T, Tasaki A, Horiuchi S, Osakabe C, Ohde S, Saida Y, et al. Quantification of fatty degeneration within the supraspinatus muscle by using a 2-point Dixon method on 3-T MRI. AJR Am J Roentgenol 2015;205:116-22. http://dx.doi.org/10.2214/AJR.14.13518

34. Oh JH, Chung SW, Kim SH, Chung JY, Kim JY. 2013 Neer award: effect of the adipose-derived stem cell for the improvement of fatty degeneration and rotator cuff healing in rabbit model. J Shoulder Elbow Surg 2014;23:445-55. http://dx.doi.org/10.1016/j.jse.2013.07.054

35. Palumbo C, Rovesta C, Ferretti M. Striated muscle fiber apoptosis after experimental tendon lesion in a rat model. J Anat 2012;221:358-63. http://dx.doi.org/10.1111/j.1469-7580.2012.01554.x

36. Penner G, Gang G, Sun X, Wray C, Hasselgren PO. C/EBP DNA-binding activity is upregulated by a glucocorticoid-dependent mechanism in septic muscle. Am J Physiol Regul Integr Comp Physiol 2002;282:R439-44. http://dx.doi.org/10.1152/ajpregu.00512.2001

37. Pirinen E, Cantó C, Jo YS, Morato L, Zhang H, Menzies KJ, et al. Pharmacological Inhibition of poly(ADP-ribose) polymerases improves fitness and mitochondrial function in skeletal muscle. Cell Metab 2014;19:1034-41. http://dx.doi.org/10.1016/j.cmet.2014.04.002

38. Reed SA, Sandesara PB, Senf SM, Judge AR. Inhibition of FoxO transcriptional activity prevents muscle fiber atrophy during cachexia and induces hypertrophy. FASEB J 2012;26:987-1000. http://dx.doi.org/10.1096/fj.11-189977

39. Ríos R, Carneiro I, Arce VM, Devesa J. Myostatin is an inhibitor of myogenic differentiation. Am J Physiol Cell Physiol 2002;282:C993-9. http://dx.doi.org/10.1152/ajpcell.00372.2001

40. Sakamaki JI, Daitoku H, Yoshimochi K, Miwa M, Fukamizu A. Regulation of FOXO1-mediated transcription and cell proliferation by PARP-1. Biochem Biophys Res Commun 2009;382:497-502. http://dx.doi.org/10.1016/j.bbrc.2009.03.022

41. Schmutz S, Fuchs T, Regenfelder F, Steinmann P, Zumstein M, Fuchs B. Expression of atrophy mRNA relates to tendon tear size in supraspinatus muscle. Clin Orthop Relat Res 2009;467:457-64. http://dx.doi.org/10.1007/s11999-008-0565-0

42. Sishi BJ, Engelbrecht AM. Tumor necrosis factor alpha (TNF-alpha) inactivates the PI3-kinase/PKB pathway and induces atrophy and apoptosis in L6 myotubes. Cytokine 2011;54:173-84. http://dx.doi.org/10.1016/j.cyto.2011.01.009

43. Wang ZQ, Auer B, Stingl L, Berghammer H, Haidacher D, Schweiger M, et al. Mice lacking ADPRT and poly(ADP-ribosyl)ation develop normally but are susceptible to skin disease. Genes Dev 1995;9:509-20.

44. Yu SW, Andrabi SA, Wang H, Kim NS, Poirier GG, Dawson TM, et al. Apoptosis-inducing factor mediates poly(ADP-ribose) (PAR) polymer-induced cell. Proc Natl Acad Sci U S A 2006;103:18314-9. http://dx.doi.org/10.1073/pnas.0606528103

45. Zanou N, Gailly P. Skeletal muscle hypertrophy and regeneration: interplay between the myogenic regulatory factors (MRFs) and insulin-like growth factors (IGFs) pathways. Cell Mol Life Sci 2013;70:4117-30. http://dx.doi.org/10.1007/s00018-013-1330-4

46. Zumstein MA, Jost B, Hempel J, Hodler J, Gerber C. The clinical and structural long-term results of open repair of massive tears of the rotator cuff. J Bone Joint Surg Am 2008;90:2423-31. http://dx.doi.org/10.2106/JBJS.G.00677